ANALYZING DAILY BEHAVIORAL DATA FOR PERSONALIZED HEALTH MANAGEMENT

An Undergraduate Research Scholars Thesis

by

RANDY ARDYWIBOWO

Submitted to the Undergraduate Research Scholars program at
Texas A&M University
in partial fulfillment of the requirements for the designation as an

UNDERGRADUATE RESEARCH SCHOLAR

Approved by Research Advisor: Dr. Xiaoning Qian

May 2017

Major: Electrical Engineering

TABLE OF CONTENTS

ABSTRACT

Analyzing Daily Behavioral Data for Personalized Health Management

Randy Ardywibowo
Department of Electrical and Computer Engineering
Texas A&M University

Research Advisor: Dr. Xiaoning Qian
Department of Electrical and Computer Engineering
Texas A&M University

Emerging wearable and environmental sensor technologies provide health professionals with unprecedented capacity to continuously collect human behavior data for health monitoring and management. This enables new solutions to mitigate globally emerging health problems such as obesity. With such outburst of dynamic sensor data, it is critical that appropriate mathematical models and computational analytic methods are developed to translate the collected data into an accurate characterization of the underlying health dynamics, enabling more reliable personalized monitoring, prediction, and intervention of health status changes. However, several challenges arise in translating them effectively into personalized activity plans. Besides common analytic challenges that come from the missing values and outliers often seen in sensor behavior data, modeling the complex health dynamics with potential influence from human daily behaviors also pose significant challenges.

We address these challenges as follows: We firstly explore existing missing value imputation and outlier detection preprocessing methods. We compare these methods with a recently developed dynamic system learning method – SSMO – that learns a personalized behavior model from real-world sensor data while simultaneously estimating missing values and detecting outliers. We then

focus on modeling heterogeneous dynamics to better capture health status changes under different conditions, which may lead to more effective state-dependent intervention strategies. We implement switching-state dynamic models with different complexity levels on real-world daily behavior data. Finally, we conducted evaluation experiments of these models to demonstrate the importance of modeling the dynamic heterogeneity, as well as simultaneously conducting missing value imputation and outlier detection in achieving better prediction of health status changes.

DEDICATION

This thesis is dedicated to all my friends, colleagues, professors, and advisors in Texas A&M University. Thank you for all the fond memories and life lessons that you all have given to me.

ACKNOWLEDGEMENTS

I would like to thank my research advisor, Dr. Xiaoning Qian, and my colleagues in his research group for their guidance and support throughout the course of this research. I also thank my friends and colleagues for making my time in Texas A&M University a great experience, and for showing me the value of being passionate in any project, research, or endeavor. Finally, thanks to my father, mother, and brother for the love and care that they provide to me.

NOMENCLATURE

AR	Auto-Regressive
ARMA	Auto-Regressive Moving Average
BCD	Block Coordinate Descent
BMI	Body Mass Index
EM	Expectation Maximization
FDA	Functional Data Analysis
FPCA	Functional Principal Component Analysis
FVE	Fraction of Variance Explained
GP	Gaussian Process
HMM	Hidden Markov Model
KKT	Karush-Kuhn-Tucker
KL	Kullback-Leibler
MLE	Maximum Likelihood Estimates
PACE	Principal Component Analysis through Conditional Expectation
PCA	Principal Component Analysis
RL	Reinforcement Learning
RMSE	Residual Mean Square Error
SAR	Switching-state Auto-Regressive
SLDS	Switching Linear Dynamical System
SSMO	System identification with Simultaneous Missing value estimation, and Outlier Detection

CHAPTER I

INTRODUCTION

Currently, obesity is considered a public health issue as over one-third of the US adult population is classified as obsess [9]. However, addressing obesity is believed to be currently beyond the capacity of the healthcare industry [13], motivating the development of smart and scalable health solutions that can automate personalized activity planning.

Smart health solutions are becoming ever more feasible with the rapid development of sensors and mobile applications that can continuously collect human behavior data such as physical activity, food intake, and Body Mass Index (BMI) [5]. However, with such outburst of dynamic sensor data, several challenges arise in translating them into personalized activity plans effectively. Besides common challenges in analyzing sensor behavior data, such as missing values and outliers, modeling the complex health dynamics with potential influence from human daily behaviors also pose significant challenges.

We explore existing methods that firstly preprocess the missing values and outliers. The preprocessing methods we explored include off-the-shelf missing value imputation and outlier detection methods, such as mean imputation and median filters, as well as analytic methods based on functional data analysis methods, such as Functional Principal Component Analysis (FPCA) [12, 17]. We compare these methods with a recently developed dynamic system learning method – SSMO – that learns a personalized behavior model from real-world sensor data while simultaneously estimating missing values and detecting outliers. We show that SSMO is superior to the other benchmarked methods with better prediction accuracy for future BMI trajectory.

We implement a Switching-state Auto-Regressive (SAR) population model [1] to capture the complex interactions of human daily behaviors. We have adopted this model framework due to its capability to capture instantaneous changes in human activity and to classify inherent health stages in a population. We compare our model to a SSMO, which does not consider these factors, showing that considering the switching-state behavior and population-wide effects improves the model's prediction performance significantly.

Borrowing from SSMO, we simultaneously consider missing value imputation and outlier detection while conducting the SAR population model identification. We compare our simultaneous imputation and outlier detection method with the aforementioned preprocessing approaches, showing that integrating missing value imputation and outlier detection with SAR population model identification significantly improves model accuracy. These experiments show improved prediction accuracy of BMI changes with different daily activity profiles.

In addition to deriving personalized health management, the proposed system is generally useful for dynamic modeling with big and low-quality data and their translation into healthcare decision making outside of clinical settings. With appropriate infrastructure, it will have a profound impact on deriving effective smart and connected health solutions using emerging mobile sensors and applications.

CHAPTER II

MISSING VALUE IMPUTATION AND OUTLIER DETECTION METHODS

Introduction

As shown in Figure 1, missing values and outliers are very abundant in daily behavior sensor data. These defects, if not addressed appropriately, could seriously degrade the accuracy of system identification and further affect activity planning. Possible effects include loss of precision due to fewer data, computational difficulties due to holes in the dataset, and bias due to distortion of the data distribution [14]. Most existing time series models in statistics literature often rely on the assumption that the time series data are complete. These models include the ARMA (Auto-Regressive Moving-Average) models and their extensions, spectral analysis methods, and state space models [3, 7, 10, 16]. Typically, a preprocessing step is used to remove these data defects in order to use these existing time series models. Popular preprocessing methods include mean value fitting, cubic fitting, and polynomial fitting for missing value estimation, and median filtering for outlier removal [14]. However, these methods are based on very different assumptions from our problem setting.

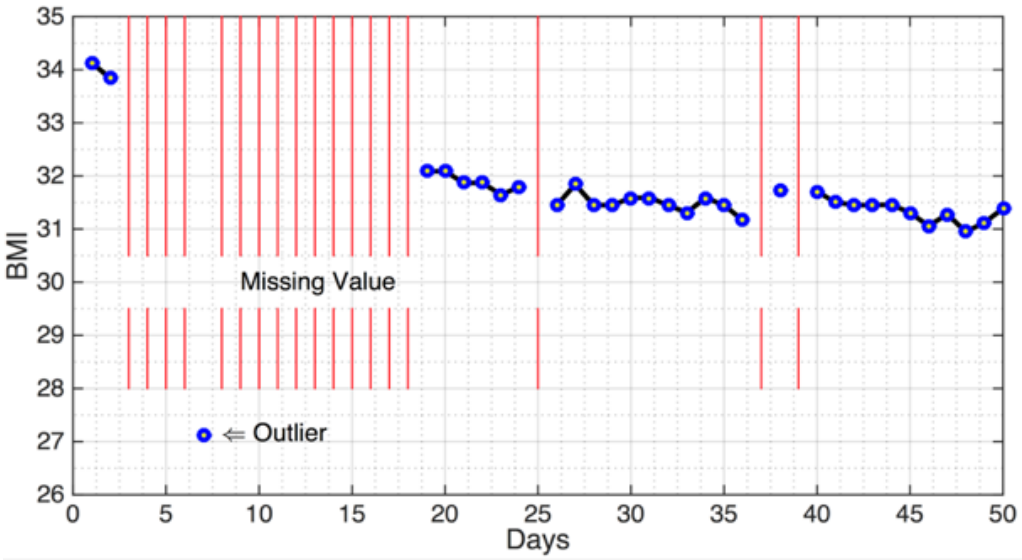

Figure 1. A typical example of life behavior data from mobile sensors

To address these issues encountered in mobile sensor data analysis, we evaluate a recently developed linear dynamic system identification engine, SSMO [18]. This engine can simultaneously address the issues of missing values and outliers while conducting model identification. We carry out a comprehensive performance evaluation of SSMO with both parametric and non-parametric Functional Data Analysis (FDA) methods, including Functional Principal Component Analysis (FPCA) with different basis functions and Principal Component Analysis through Conditional Expectation (PACE), as well as other off-the-shelf missing value and outlier detection methods, showing that SSMO is superior to the other benchmarked methods. This evaluation provided insight into developing a daily behavioral data model with a solution strategy similar to SSMO.

Dynamic System Identification with Simultaneous Missing Value Estimation, and Outlier Detection (SSMO)

The dynamic system learning method, SSMO, can automatically remove the effects of potential outliers in the dataset, fill in missing values, and conduct model identification [18]. To introduce

this method, let $\{x_t, u_t\}_{t=1}^{T}$ denote a given a user record with a series of observations, where x_t denotes the outcome at time t and u_t denotes the behavior profile at time t. SSMO adopts a linear dynamic system as the underlying model to characterize the relationships between the behavioral variables and outcome variables. In our study on obesity, the outcome variable is BMI while the behavioral variables include calorie intake (food), calories burned during workout or exercise, and workout time. The linear dynamic system is a flexible model that can characterize a wide range of dynamics. For instance, the following linear dynamic system can model the 3rd-order dynamics:

$$\begin{bmatrix} x_{t+1} \\ x_t \\ x_{t-1} \end{bmatrix} = A \begin{bmatrix} x_t \\ x_{t-1} \\ x_{t-2} \end{bmatrix} + B \begin{bmatrix} u_t \\ u_{t-1} \\ u_{t-2} \end{bmatrix} + C + \boldsymbol{w}_t \quad (1)$$

Here, $\boldsymbol{w}_t$ is white noise, and C is a bias term. This formulation can capture both spontaneous effects and delayed effects. When needed, the model can be extended to include higher order dynamics.

SSMO is formulated as follows: let $X = [\mathrm{x}_0, \mathrm{x}_1, \dots, \mathrm{x}_T]$ be the state matrix and $U = [\mathrm{u}_0, \mathrm{u}_1, \dots, \mathrm{u}_{T-1}]$, be the action matrix. Let Ω_x and Ω_u be the set of observable elements of X and U respectively. Furthermore, let $\hat{X} = [\hat{\mathrm{x}}_0, \hat{\mathrm{x}}_1, \dots, \hat{\mathrm{x}}_T]$ and $\hat{U} = [\hat{\mathrm{u}}_0, \hat{\mathrm{u}}_1, \dots, \hat{\mathrm{u}}_{T-1}]$ denote the estimates of X and U. SSMO's systems identification is formulated as the following optimization problem:

$$\min_{A,B,C,\hat{X},\hat{U}} \ \frac{1}{2}\sum_{t=0}^{T-1} \left\| \begin{bmatrix} \hat{x}_{t+1} \\ \hat{x}_t \\ \hat{x}_{t-1} \end{bmatrix} - \left(A \begin{bmatrix} \hat{x}_t \\ \hat{x}_{t-1} \\ \hat{x}_{t-2} \end{bmatrix} + B \begin{bmatrix} \hat{u}_t \\ \hat{u}_{t-1} \\ \hat{u}_{t-2} \end{bmatrix} + C \right) \right\|^2 \quad (2a)$$

$$\text{s.t.} \quad \left\| \left(\hat{X} - X\right)_{\Omega_x} \right\|_0 \le \eta_x, \left\| \left(\hat{U} - U\right)_{\Omega_u} \right\|_0 \le \eta_u \quad (2b)$$

The objective function $(2a)$ is a squared loss function to evaluate the goodness-of-fit of the parameters A, B, and C, as well as $\hat{X}$ and $\hat{U}$. The constraints $(2b)$ serve to limit the maximum number of outliers to be detected in X and U, while the values of η_x and η_u can be estimated by the upper bound of the percentage of outliers [18].

SSMO Solution Strategy by Block Coordinate Descent (BCD)

Block Coordinate Descent (BCD) [15] was used to solve (2) by alternatively optimizing two groups of variables: $\{A, B, C\}$ and $\{\hat{X}, \hat{U}\}$. $\{A, B, C\}$ can be optimized through standard least squares optimization, admitting a closed-form solution. To optimize $\{\hat{X}, \hat{U}\}$, we adopt the projected gradient descent method to iteratively update $\hat{X}_i^{k+1} = \arg\min_{\hat{X}_i} \left\{ \left\| \hat{X} - \left(\hat{X}^k - \Delta g_{\hat{X}^k} \right) \right\|_F^2 \right\}$, where $g_{\hat{X}^k}$ is the partial derivative of the objective function (2a) w.r.t. $\hat{X}^k$, Δ is the step size that could be chosen to be a sufficiently small constant, and $\|\cdot\|_F$ denotes the Frobenius norm. The update for $\hat{U}$ follows a similar procedure. The optimization procedure is summarized in Algorithm 1.

Algorithm 1 BCD for SSMO

Input: $X_{\Omega_x}, U_{\Omega_x}, \eta_x, \eta_u$
Output: $A, B, C, \hat{X}, \hat{U}$
While (not converged)
  Optimize A, B, C by minimizing the least squares problem (2a) without any constraint.
  Optimize $\hat{X}$: Select top η_x elements in
    $\left(\hat{X} - X - \Delta g_{\hat{X}}\right)_{\Omega_x}$ forming the index set Z_X.
    $\left(\hat{X}\right)_{\overline{\Omega}_x \cup Z} \leftarrow \left(\hat{X} - \Delta g_{\hat{X}}\right)_{\overline{\Omega}_x \cup Z_X}$
  Optimize $\hat{U}$: Select top η_u elements in
    $\left(\hat{U} - U - \Delta g\right)_{\Omega_u}$ forming the index set Z.
    $\left(\hat{U}\right)_{\overline{\Omega}_u \cup Z_U} \leftarrow \left(\hat{U} - \Delta g_{\hat{U}}\right)_{\overline{\Omega} \cup Z_U}$
End
Return $A, B, C, \hat{X}, \hat{U}$

Functional Data Analysis (FDA)

Instead of solving (2) for simultaneous missing value imputation and system learning, we test other missing value imputation methods and evaluate them based on the prediction accuracy of future trajectory. We are specifically interested in missing value imputation methods for Functional Data Analysis (FDA) [12] for studying time series data as in our application.

Functional Principal Component Analysis with Different Base Functions

We explore Functional Data Analysis (FDA) with different base functions for handling missing values and outliers before systems learning using our SSMO engine. In the FDA framework, given a vector of observations $\boldsymbol{y}$, we estimate the underlying function $\boldsymbol{x}$ by the penalized least squares smoothing method as formulated to minimize the following loss function [12]:

$$\mathrm{PENSSE}_m(\boldsymbol{y}|\boldsymbol{c}) = (\boldsymbol{y} - \boldsymbol{\Phi c})'\mathbf{W}(\boldsymbol{y} - \boldsymbol{\Phi c}) \quad (3a)$$
$$+ \lambda \times \mathrm{PEN}_m(x)\,. \quad (3b)$$

Noting that the underlying function $\boldsymbol{x}$ is expressed in a different basis system as $\boldsymbol{x} = \boldsymbol{\Phi c}$, where $\boldsymbol{\Phi}$ is the basis matrix and $\boldsymbol{c}$ is the coefficients representing $\boldsymbol{x}$ in the basis system defined by $\boldsymbol{\Phi}$, we can see that $(3a)$ is a weighted least squares estimation. The roughness penalty term $(3b)$ is added to enforce smoothness on the estimation of $\boldsymbol{x}$, with λ being a penalty coefficient, and $\mathrm{PEN}_m(\boldsymbol{x})$ as the square integration of the m^{th} derivative, a measure of a function's roughness. This function is denoted as follows:

$$\mathrm{PEN}_m(x) = \int [D^m x(s)]^2 ds\,. \quad (4)$$

The order of derivative typically penalized here is the second or fourth order derivative [12]. We can subsequently substitute $\boldsymbol{\Phi c}$ for $\boldsymbol{x}$ and express this roughness penalty in matrix form as follows:

$$\mathrm{PEN}_m(x) = c'\mathbf{R}c \quad (5)$$

$$\mathbf{R} = \int D^m\phi(s) D^m\phi(s)' ds\,. \quad (6)$$

Note that the loss function (3) is convex and solving this model leads to closed-form solutions by the Karush-Kuhn-Tucker (KKT) conditions, similar to classic ordinary or weighted least squares problems [12]. The weighting for smoothness penalty can be determined by dividing the

training dataset and performing cross validation, using the penalty parameter that produces the best estimation accuracy within the cross-validation testing.

The smoothness assumptions of the estimated behavioral data may change as different variables have varying degrees of smoothness, such as BMI vs. the calories the user has burned in a day. To comprehensively evaluate the performance, two different basis systems were explored with this method, the B-spline basis and Haar wavelet basis. These basis systems were chosen due to their stark contrasts, with the B-spline basis offering the smoothest estimation while the Haar basis can capture abrupt changes in the data.

B-spline Basis

The B-spline basis is a basis system that represents functional data as a combination of piecewise spline functions of a certain degree k, with the corresponding polynomials approximating the function along with their derivatives up to $k-1$ are constrained to be equal at these breakpoints or knots. This produces a smooth representation of the behavioral data. To accommodate for abrupt changes that may happen in behavioral data, multiple knots may be placed in a single time point.

The equation for a spline function is as follows. Let $B_i(t,\tau)$, be a piecewise polynomial function defined by the breakpoint sequence τ, with i being the number of the largest knot positioned less than or equal to t. Let K be the total number of subintervals used. Then, the spline function $S(t)$ is defined as follows:

$$S(t) = \sum_{1 \le k \le K} c_k B_k(t,\tau) \qquad (7)$$

Haar Wavelet Basis

The Haar wavelet basis is a basis formed by a sequence of square-shaped functions [6]. Its mother wavelet $\psi(t)$ and scale function $\phi(t)$ are described as follows:

$$\psi(t) = \begin{cases} 1 & 0 \le t < \frac{1}{2} \\ -1 & \frac{1}{2} \le t < 1 \\ 0 & \text{otherwise} \end{cases} \quad (8a)$$

$$\phi(t) = \begin{cases} 1 & 0 \le t < 1 \\ 0 & \text{otherwise} \end{cases} \quad (8b)$$

The mother wavelet and scale function represents the basis system by different dilations and translations n and k respectively, represented by the following equation:

$$\psi_{n,k}(t) = 2^{n/2}\psi(2^n t - k) \quad (9)$$

This function is put into the basis matrix $\mathbf{\Phi}$, with the columns being a basis formed by certain nonnegative integer n and $0 \le k \le 2^j - 1$.

Principal Component Analysis through Conditional Expectation (PACE)

Designed for analyzing sparse data, the PACE model is a non-parametric model and gives estimations of data from an individual subject by also considering data from the entire collection of subjects. This gives the best approximation of a function represented as a linear combination of k functional curves.

Formulated similarly to the aforementioned Functional Principal Component Analysis (FPCA) methods, the data, $X(t)$ is modelled as noisy sampled points from a collection of trajectories that are assumed to be independent realizations of a smooth random function, with unknown mean function $\mathrm{E}[X(t)] = \mu(t)$ and covariance function $\mathrm{cov}\big(X(s), X(t)\big) = G(s,t)$. The domain of $X(t)$ is bounded on a closed time interval T. Assuming an L^2 orthogonal expansion of G exists in terms of eigenfunctions ϕ_k and eigenvalues λ_k: $G(s,t) = \sum_k \lambda_k \phi_k(s)\phi_k(t)$, the i^{th} user's trajectory can be represented as $X_i(t) = \mu(t) + \sum_k \xi_{ik}\phi_k(t), t \in T$, where ξ_{ik} are uncorrelated random variables with zero mean. By also incorporating uncorrelated measurement errors, the model considered becomes

$$Y_{ij} = X_i(T_{ij}) + \epsilon_{ij} = \mu(T_{ij}) + \sum_{k=1}^{\infty} \xi_{ik}\phi_k(T_{ij}) + \epsilon_{ij} \qquad T_{ij}\,\epsilon\,T, \qquad (10)$$

Where ϵ_{ij} are uncorrelated measurement errors with mean zero and constant variance σ^2, and Y_{ij} is the j^{th} observable data point of the i^{th}user.

To accommodate for the sparsity of daily behavioral data, local linear smoothers are used to estimate the mean function $\mu(t)$, instead of traditionally taking the average at each time point. This is because, in addition to being sparse, the time points of each user data may also not align with each other, causing bias in estimating the mean function through averaging. Estimation of the variance σ^2, is done through estimation of the covariance surface $\mathrm{cov}(X(T_{ij}),X(T_{il}))$. A linear fit is used to estimate the diagonal elements of the covariance matrix, while a local quadratic fit is used for the off diagonal elements, as the covariance matrix is maximal along its diagonal. The eigenfunctions can be subsequently found by discretizing the smoothed covariance surface. In these steps, we utilized the Gaussian kernel to perform the implicit feature mapping of the smooth surface estimation.

As a novelty introduced in the PACE formulation, the principal component scores are estimated by conditioning over the observations $\boldsymbol{Y}_i$, rather than through numeric integration of the FPCA integral transform commonly used in traditional FPCA [17]. Compared to traditional FPCA, this is more suitable for sparse data as not enough points are available to perform a numeric integration. This is estimated by the following equation:

$$\hat{\xi}_{ik} = \hat{E}\left[\xi_{ik}\middle|\widehat{\boldsymbol{Y}}_i\right] = \hat{\lambda}_k \hat{\boldsymbol{\phi}}_{ik}^T \widehat{\boldsymbol{\Sigma}}_{Y_i}^{-1}\left(\widetilde{\boldsymbol{Y}}_i - \widetilde{\boldsymbol{\mu}}_i\right) \qquad (11)$$

With $\hat{\lambda}_k$, $\hat{\boldsymbol{\phi}}_{ik}$, and $\widehat{\boldsymbol{\Sigma}}_{Y_i}$ being the estimates of λ_k, $\boldsymbol{\phi}_{ik}$, and $\boldsymbol{\Sigma}_{Y_i}$, the covariance matrix of $\boldsymbol{Y}_i$, respectively [2]. We apply this formulation for each measured variable separately, estimating the

model described above for each type of measured data (calories burned, calories consumed, workout time, workout calories, and BMI).

CHAPTER III

MISSING VALUE IMPUTATION AND OUTLIER DETECTION METHOD EVALUATIONS

Off-the-shelf Missing Value Imputation and Outlier Detection Methods

In addition to the methods we detailed in Chapter 2, we also test several off-the-shelf imputation methods, including the last value carried forward method and mean imputation method. These methods impute missing values by taking the last value observed in the data and the mean of the data respectively. To detect outliers with these methods, we utilize a median filter before imputing the data.

Among the missing values and outlier detection approaches we benchmarked, the off-the-shelf missing value and outlier detection methods performed the worst based on future BMI prediction accuracy. The "mean imputation" method ignores the context as it fails to utilize the underlying dynamics of the variables. On the other hand, the "last value carried forward" method takes a conservative approach, underestimating the changes over time. Thus, neither method is suitable for imputing missing values in dynamic modeling context.

PCA with B-spline Basis

In estimating each user's behavioral data, 4^{th} order splines were used while imposing a roughness penalty on its second derivative. The penalty on second derivative as well as the use of B-splines produce a smooth representation of the behavioral trajectories as shown in Figure 2.

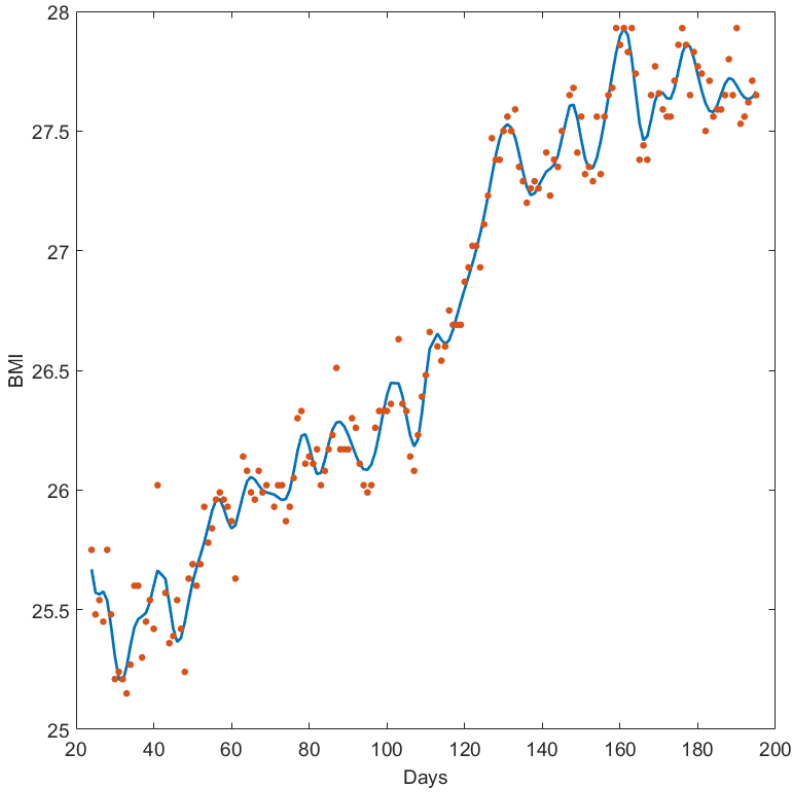

Figure 2. Missing value estimation and outlier detection using FPCA with B-spline basis

PCA with Haar Wavelet Basis

This basis system was utilized with no roughness penalty term, reducing the estimation problem into a weighted least squares problem. The use of the Haar Wavelet basis captures the instantaneous changes in daily behavior trajectories as shown in Figure 3. A comparison of both basis function representations is shown in Figure 4.

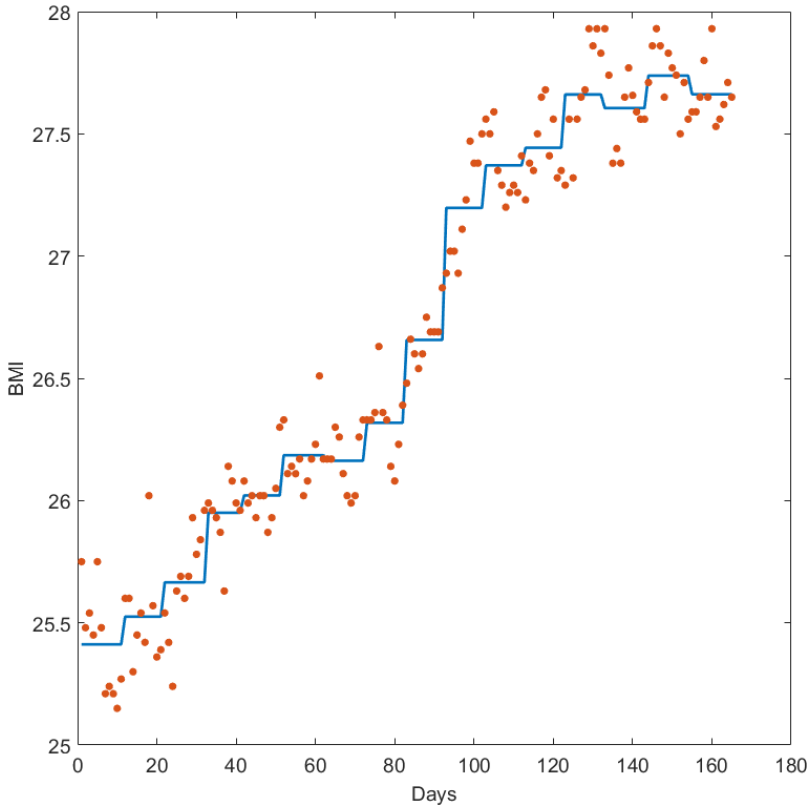

Figure 3. Missing value estimation and outlier detection using FPCA with Haar wavelet basis

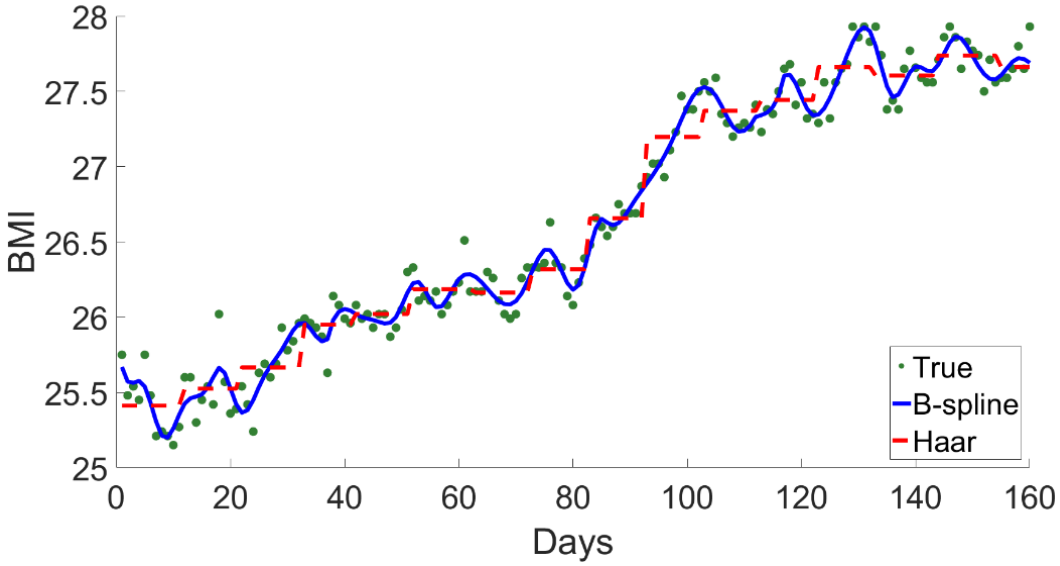

Figure 4. Missing value estimation and outlier detection using FPCA with B-spline and Haar wavelet basis

Principal Component Analysis through Conditional Expectation (PACE)

As the PACE method is non-parametric, no assumptions are made on the underlying distribution of the daily behavioral trajectory. This allows the method to adapt to each trajectories smoothness and instantaneous changes accordingly. To select the number of eigenfunctions used in our model, we measure the fraction of variance explained (FVE) and picked the model which explains at least 95% of the total variation. An example of a trajectory estimated by this method is shown in Figure 5.

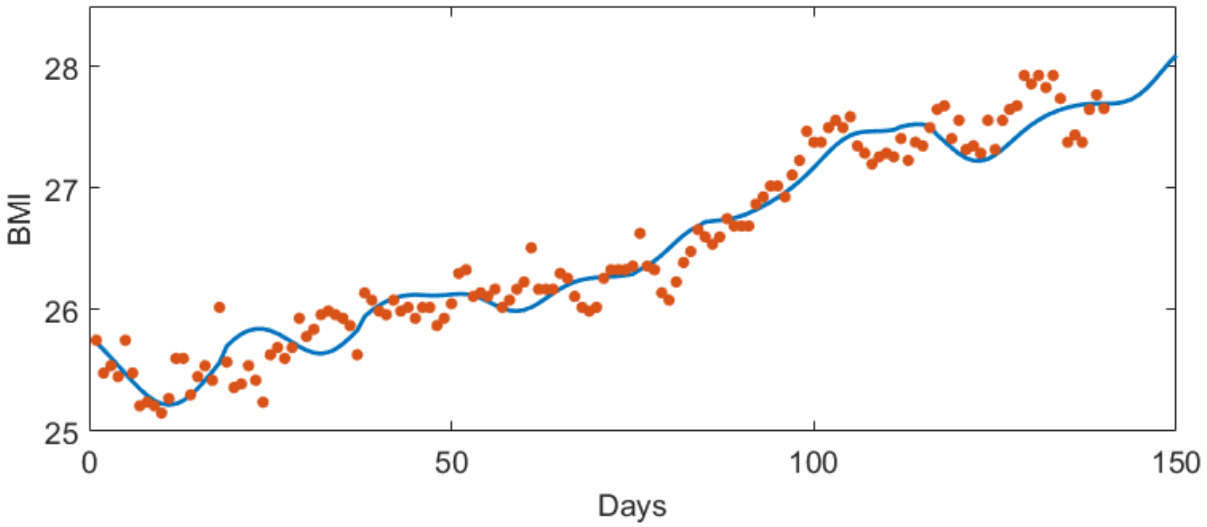

Figure 5. Missing value estimation and outlier detection using PACE

Evaluation

The methods we detailed are used on daily behavioral data from 25 different users. This daily behavioral data consists of data for calories consumed, calories burned, workout time, workout calories, and BMI taken in a daily interval. We benchmarked all the methods using both the L-1 norm error (ABS) and the Residual Mean Squared Error (RMSE) in predicting future BMI trajectory. In our tests, SSMO performed better than all the other methods we benchmarked, giving the best prediction accuracy overall, as shown in Figure 6 and Table 1. FDA-based imputation and

outlier detection methods perform better than naive off-the-shelf methods but the unified SSMO method clearly outperforms them.

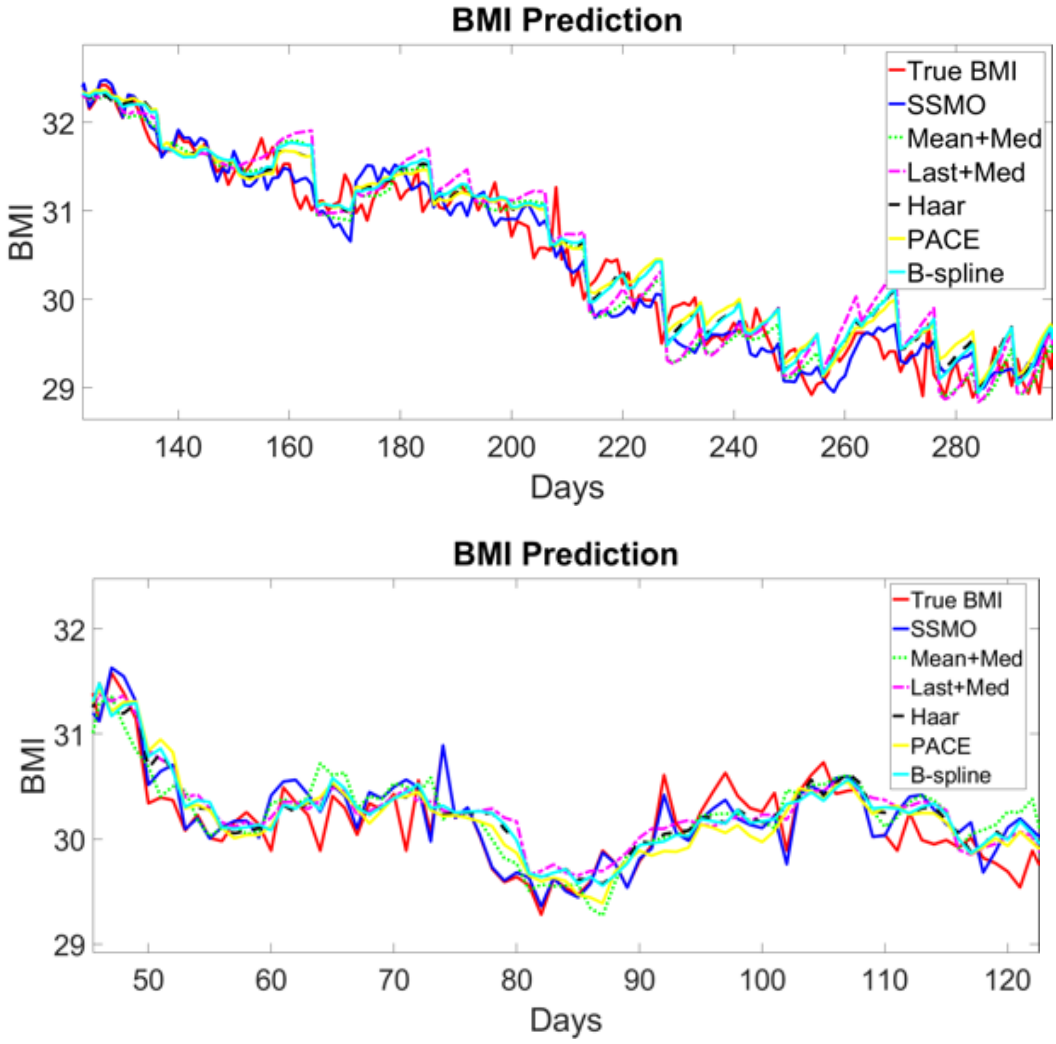

Figure 6. BMI prediction trajectory for the benchmarked imputation methods

Table 1: Evaluation results for different missing value estimation and outlier detection methods

	Mean	Last	Mean + Med	Last + Med
RMSE	1.3106 ± 2.12820	1.0597 ± 1.0590	0.7375 ± 0.6045	0.8576 ± 0.5713
ABS	1.1126 ± 1.8972	0.8705 ± 0.8541	0.5805 ± 0.5078	0.6499 ± 0.4646
	Haar	B-spline	PACE	SSMO
RMSE	0.7227 ± 0.4689	0.6952 ± 0.5164	0.7143 ± 0.5520	**0.6714 ± 0.4890**
ABS	0.5716 ± 0.3884	0.5354 ± 0.4137	0.5426 ± 0.4478	**0.5174 ± 0.3968**

CHAPTER IV

SWITCHING LINEAR DYNAMICAL SYSTEMS

Introduction

Although SSMO could predict BMI trajectory with good accuracy, the model formulation has several shortcomings when used in analyzing daily behavioral data. Firstly, SSMO models the daily behaviors of each subject separately. This treatment assumes that each subject's behavior pattern is uncorrelated to one another. However, intuitively, each subject's behavioral pattern should be correlated with each other, as similar behaviors should be linked to similar outcomes. Moreover, this assumption would make system identification intractable when dealing with many subjects, as each person's daily behavioral model would need to be identified separately under sparse data conditions for each individual.

Secondly, shown by the prediction results of SSMO, the model is unable to handle instantaneous change in BMI, leading to inaccurate short-term predictions. This is a critical issue, as daily behavioral data features many instantaneous changes. Moreover, as the main proposed application of this system is in active health monitoring, failure to account for these instantaneous changes could lead to dangerous false negatives in monitoring health trajectory.

Finally, a desirable result in modeling daily behaviors is to classify subjects into groups of different health statuses. This feature would make disease detection possible as different disease stages can be inferred by the current states of each patient. Because SSMO assumes no correlation between each subject's daily behavioral system, this feature can't be achieved with its current formulation.

A class of models that could mitigate the shortcomings of SSMO and achieve features mentioned above is the class of Switching Linear Dynamical Systems (SLDS). These dynamic models incorporate a discrete switching variable that serves to divide temporal data into segments, each modelled by a different linear dynamical system. From this class of systems, a population model can be derived. This is done by assuming that the states of each subject at any given time belong to a set of states shared across all subjects.

The SLDS population model has several advantages over SSMO. Firstly, unlike SSMO, the SLDS population model correlates each subject's behavior pattern that of other subjects through its shared state. This assumption is not only intuitive, but also makes the problem more computationally tractable when modeling many subjects' health trajectory. Secondly through its switching behavior, the model is capable of handling instantaneous changes in human behavior. Finally, the model can classify subjects into groups of different health statuses. This can be achieved by noting that different subjects would tend towards different sets of switching states, allowing the use of classification algorithms to discriminate between subjects of different groups. Because of this, we explore the Switching-state Auto-Regressive (SAR) model formulated as a population model.

Switching-state Auto-Regressive (SAR) Population Model Formulation

We implement a Switching-state Auto-Regressive (SAR) population model in our analysis of the daily behavioral data set. To model the potential heterogeneous dynamic changes of health status, we consider the underlying dynamic system can switch from time to time under different conditions. For the i^{th} subject ($i \in \{1, \dots, N\}$) at time t, we assume that there exists a discrete latent health state s_t^i determining the dynamics of a health indicator, represented by x_t^i, as well as the influence from input variables capturing daily life behavior, denoted by u_t^i.

Specifically, we are interested in the observed health indicator BMI as the health status of interest, and its change across time. The input variables include calorie intake (food), calories burned during workout or exercise, and workout time. SAR models the BMI dynamics by the following system model:

$$x_t^i = \mathbf{a}\left(s_t^i\right)^{\mathrm{T}} \mathbf{x}_{t-1}^i + \mathbf{b}\left(s_t^i\right)^{\mathrm{T}} \mathbf{u}_t^i + c\left(s_t^i\right) + \eta_t^i \quad (12a)$$

$$\eta_t^i \sim \mathcal{N}\left(0, \sigma_i^2\left(s_t^i\right)\right) \quad (12b)$$

Note that the SAR model is the extension of the classical Auto-Regressive (AR) models by allowing the system coefficients $\boldsymbol{a}(s)$, $\boldsymbol{b}(s)$, and $c(s)$ to be determined by the latent health state s. In general, the system in (12) can incorporate any order of time lags L_x and L_u to model the potential high-order dependence relationships so that $\mathbf{x}_{t-1}^i$ and $\mathbf{u}_t^i$ can take the following measurements:

$$\mathbf{x}_{t-1}^i = \left[x_{t-1}^i, x_{t-2}^i, \ldots, x_{t-L_x}^i\right]^{\mathrm{T}} \quad (13a)$$

$$\mathbf{u}_t^i = \left[u_t^i, u_{t-1}^i, \ldots, u_{t-L_u+1}^i\right]^{\mathrm{T}} \quad (13b)$$

We adopt a ***population SAR model*** assuming that the system coefficients $\boldsymbol{a}(s)$, $\boldsymbol{b}(s)$, and $c(s)$ are shared between subjects while each subject has independent measurement noise variance $\sigma_i^2(s)$. For the case with $L_x = L_u = 1$, the population SAR model is illustrated in Figure 7:

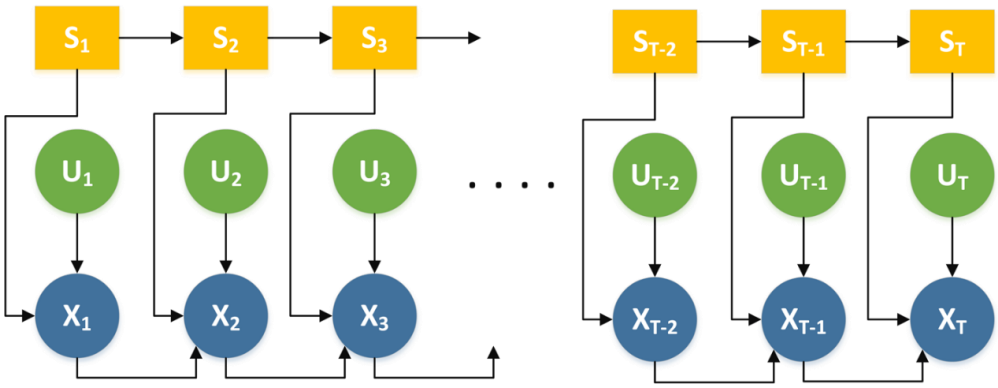

Figure 7: First-order SAR model

It has a finite Markov chain layer to model the health state changes along time and an AR model layer to capture the "controlled" dynamic changes at different health states.

To learn the SAR model given the observed daily behavior data and BMI changes, we have the following auto-regressive coefficients as well as health states to identify:

$$\boldsymbol{\theta} = \{\mathbf{a}(s), \mathbf{b}(s), c(s), \sigma_i^2(s), s \in \{1, \dots, S\}, i \in \{1, \dots, N\}\}. \quad (14)$$

As each subject's time series measurements are independent of each other given the population SAR model, we have the following likelihood function of the population SAR model given observed data:

$$p(x_{1:N\times 1:T}, s_{1:N\times 1:T} | u_{1:N\times 1:T}, \boldsymbol{\theta}) = \prod_{i=1}^{N} p_i(X_i, S_i | U_i, \boldsymbol{\theta}) \quad (15a)$$

$$p_i(X_i, S_i | U_i, \boldsymbol{\theta}) = \prod_{t=1}^{T} p(x_t | \hat{\mathbf{x}}_{t-1}, \hat{\mathbf{u}}_t, s_t, \boldsymbol{\theta}) p(s_t | s_{t-1}) \quad (15b)$$

Learning the SAR Model

To derive the maximum likelihood estimates (MLE) for model identification, Expectation-Maximization (EM) is adopted to find the set of system coefficients and variances $\mathbf{a}(s)$, $\mathbf{b}(s)$, $c(s)$, and $\sigma_i^2(s)$ for all $s \in \{1, \dots, S\}$. This method alternates between estimating the state conditional probabilities $p(s_t^i | x_{1:T}^i, u_{1:T}^i)$ and optimizing the system coefficients based on the estimated state probabilities in the expectation and maximization steps respectively.

E-Step

The expectation step is done by the Forward-Backward algorithm, which estimates the state probability $p(s_t^i | x_{1:T}^i, u_{1:T}^i)$ by combining partial solutions conditioned on past and future observations with respect to t. The partial solutions conditioned on past observations are denoted

by $\alpha(s_t^i) = p(s_t^i|x_{1:t}^i, u_{1:t}^i)$, while the partial solutions for future observations are denoted by $\beta(s_{t-1}^i) = p(x_{t:T}^i|s_{t-1}^i, u_{t:T}^i)$. Given the model, we denote $p(x_t^i|s_t^i, \mathbf{x}_{t-1}^i, \mathbf{u}_t^i)$ by $\hat{p}(x_t^i|s_t^i)$:

$$\hat{p}_i(x_t^i|s_t^i) \sim \mathcal{N}\left(\mathbf{a}(s_t^i)^{\mathrm{T}}\mathbf{x}_{t-1}^i + \mathbf{b}(s_t^i)^{\mathrm{T}}\mathbf{u}_t^i + c(s_t^i), \sigma_i^2(s_t^i)\right) \quad (16)$$

Define the log-likelihood $L(\boldsymbol{\theta}) = \log\left(\sum_i \sum_t \alpha(s_t^i)\right)$ with $\alpha(s_1^i) = p(s_1^i, x_1^i|\mathbf{x}_0^i, \mathbf{u}_1^i, \boldsymbol{\theta})$, which can be solved as a filtering problem by the α-recursion [11]:

$$\alpha(s_t^i) = p(x_t^i|s_t^i, \mathbf{x}_{t-1}^i, \mathbf{u}_t^i, \boldsymbol{\theta}) \sum_{s_{t-1}^i} p(s_t^i|s_{t-1}^i)\, \alpha(s_{t-1}^i). \quad (17)$$

On the other hand, the partial solution conditioned on future observations can be solved using the β-recursion:

$$\beta(s_{t-1}^i) = \sum_{s_t^i} p(x_t^i|s_t^i, \mathbf{x}_{t-1}^i, \mathbf{u}_t^i, \boldsymbol{\theta}) p(s_t^i|s_{t-1}^i)\, \beta(s_t^i), \quad (18)$$

and $\beta(s_T^i) = 1$. By Bayes' rule, combining these two partial results yields the desired state probability:

$$\gamma(s_t^i) = p(s_t^i|x_{1:T}^i, u_{1:T}^i, \boldsymbol{\theta}) = \frac{\alpha(s_t^i)\beta(s_t^i)}{\sum_{s_t^i} \alpha(s_t^i)\beta(s_t^i)}. \quad (19)$$

Because each subject's time series is independent with one another, the expectation step can be done independently on each subject. Finally, we can derive the joint state transition probability by normalization with

$$p(s_t^i, s_{t+1}^i|x_{1:T}^i, u_{1:T}^i, \boldsymbol{\theta}) \propto \alpha(s_t^i)\hat{p}(x_{t+1}^i|s_{t+1}^i)p(s_{t+1}^i|s_t^i)\beta(s_{t+1}^i) \quad (20)$$

M-Step

The maximization step uses the state distributions calculated in the expectation step to optimize the system coefficients by minimizing the Kullback-Leibler (KL) divergence:

$$E = \sum_i \sum_t \langle \log p\left(x_t^i \middle| \hat{\mathbf{x}}_{t-1}^i, \hat{\mathbf{u}}_t^i, \mathbf{a}(s_t^i), \mathbf{b}(s_t^i), c(s_t^i)\right)\rangle_{p^{old}(s_t^i | x_{1:T}^i)}$$

$$+ \sum_i \sum_t \langle \log p(s_t^i | s_{t-1}^i)\rangle_{p^{old}(s_t^i, s_{t-1}^i)} \quad (21)$$

Rewrite the system coefficients and variables as follows:

$$\mathbf{d}(s_t^i) = \begin{bmatrix} \mathbf{a}(s_t^i) \\ \mathbf{b}(s_t^i) \\ c(s_t^i) \end{bmatrix} \qquad \hat{\mathbf{v}}_{t-1}^i = \begin{bmatrix} \hat{\mathbf{x}}_{t-1}^i \\ \hat{\mathbf{u}}_t^i \end{bmatrix} \quad (22)$$

The KKT condition [4] to minimize the KL divergence with respect to $\mathbf{d}(s)$ leads to solving the following linear system by plugging (16) into (21):

$$\sum_i \sum_t p^{old}(s_t^i = \mathrm{s} | x_{1:T}^i) \frac{x_t^i \hat{\mathbf{v}}_{t-1}^i}{\sigma_i^2(\mathrm{s})}$$

$$= \left[\sum_i \sum_t p^{old}(s_t^i = s | x_{1:T}^i) \frac{\hat{\mathbf{v}}_{t-1}^i (\hat{\mathbf{v}}_{t-1}^i)^{\mathrm{T}}}{\sigma_i^2(\mathrm{s})}\right] \mathbf{d}(\mathrm{s}) \quad (23)$$

Similarly, σ_i^2 may be solved by the following equation:

$$\sigma_i^2(\mathrm{s}) = \frac{1}{\sum_{t'} p^{old}(s_{t'}^i = \mathrm{s} | x_{1:T})} \times$$

$$\sum_t p^{old}(s_t^i = s | x_{1:T}^i) \left[x_t^i - (\hat{\mathbf{v}}_{t-1}^i)^{\mathrm{T}} \mathbf{d}(s_t^i)\right]^2 \quad (24)$$

Simultaneous System Identification, Missing Value Imputation, and Outlier Detection (SSMO)

One of the critical challenges to learn the SAR model parameters arise from the large number of missing values and frequent outlier points in the data set. This is illustrated in a fragment of real-world time series BMI measurements in Figure 1. Inappropriate handling of missing values and outliers may lead to computational difficulties from the holes in the data set, as well as the

bias and loss of precision due to distortion of the data distribution [14]. For example, among the approaches that handle missing values [8], the mean imputation method ignores the context as it fails to utilize the underlying dynamics of the variables. The last-value-carried-forward method takes a conservative approach, underestimating the changes over time. Thus, neither method is suitable for imputing missing values in the dynamic modeling context.

Extending the SAR population model, we develop a method that can simultaneously remove outliers, impute missing values, while also conducting SAR model identification [18]. The missing value imputation and outlier detection is formulated as follows: denote the state observations and actions for subject i as $X_i = [x_0^i, x_1^i, \dots, x_T^i]$ and $U_i = [u_0^i, u_1^i, \dots, u_{T-1}^i]$ respectively. Let X_i and U_i denote the set of states and actions for subject i while Ω_{x_i} and Ω_{u_i} be the set of observable elements of X_i and U_i respectively. We estimate $\hat{X}_i = [\hat{x}_0^i, \hat{x}_1^i, \dots, \hat{x}_T^i]$ and $\hat{U}_i = [\hat{u}_0^i, \hat{u}_1^i, \dots, \hat{u}_{T-1}^i]$ for systems identification by the following optimization problem instead of directly solving (21):

$$\min_{\hat{X},\hat{U}} \sum_{i=1}^{N} \sum_{t=0}^{T-1} \left\| x_t^i - \left[\left(\hat{\mathbf{x}}_{t-1}^i\right)^{\mathrm{T}} \mathbf{a}\left(s_t^i\right) + \left(\hat{\mathbf{u}}_t^i\right)^{\mathrm{T}} \mathbf{b}\left(s_t^i\right) + c\left(s_t^i\right) \right] \right\|^2 \quad (25a)$$

$$\text{s.t.} \quad \left\| \left(\hat{X}_i - X_i\right)_{\Omega_{x_i}} \right\|_0 \le \eta_x, \left\| \left(\hat{U}_i - U_i\right)_{\Omega_{u_i}} \right\|_0 \le \eta_u \quad (25b)$$

The objective function (25a) is a squared loss function to evaluate the goodness-of-fit of the missing values and outliers of the entire data set $\hat{X}$ and $\hat{U}$. Meanwhile, the constraints (25b) serve to limit the maximum number of outliers to be detected in X and U. The values of η_x and η_u can be estimated by the upper bound of the percentage of outliers [18].

Solution Strategy

To simultaneously fit the system coefficients, estimate the state probabilities, as well as imputing missing values and removing outliers, we alternatively optimize three groups of variables: the state distributions $p(s_t^i | x_{1:T}^i, u_{1:T}^i)$, the system coefficients $\boldsymbol{\theta} = \{\mathbf{d}(s),\ \sigma_i^2(s)\}$, and

the missing value and outlier estimates $\{\hat{X}_i, \hat{U}_i\}$ for all $i \in \{1, \dots, N\}$ [15]. Calculating the state distributions and optimizing $\boldsymbol{\theta}$ can be done based on the EM algorithm. On the other hand, the missing values and outliers for each subject i are estimated using the projected gradient descent method as follows:

$$\hat{X}_i^{k+1} = \arg\min_{\hat{X}_i} \left\{ \left\| \hat{X}_i - \left(\hat{X}_i^k - \Delta g_{\hat{X}_i^k} \right) \right\|_F^2 \right\}$$
$$\text{s.t.} \quad \left\| \left(\hat{X}_i - X_i \right)_{\Omega_{x_i}} \right\|_0 \leq a \qquad (26)$$

Here, $g_{\hat{X}_i^k}$ is the partial derivative of the objective function w.r.t. $\hat{X}_i^k$, Δ is the step size that could be chosen to be a sufficiently small constant, while $\|\cdot\|_F$ denotes the Frobenius norm. The optimization procedure is done as follows: First, select η_x elements in $\left(\hat{X}_i^k - \hat{X}_i - \Delta g_{\hat{X}_i^k} \right)_{\Omega_{x_i}}$ with the largest magnitudes as the outliers at the current iteration, forming a set Z_{X_i}. Second, assign the set of missing values $\overline{\Omega}_{x_i}$ and the set of detected outliers Z_{X_i} with new estimates as follows: $\left(\hat{X}_i^{k+1} \right)_{\overline{\Omega}_{x_i} \cup Z_{X_i}} = \left(\hat{X}_i^k - \Delta g_{\hat{X}_i^k} \right)_{\overline{\Omega}_{x_i} \cup Z_{X_i}}$. The remaining elements in $\hat{X}_i^{k+1}$ are set to take the same values as $\hat{X}_i^k$. The update for $\hat{U}_i$ follows a similar procedure. The entire model identification, missing value imputation and outlier detection procedure is summarized in Algorithm 1. An example of this algorithm ran on a test dataset shown in Figure 8. With the different colors representing states, Figure 8 shows that the solution strategy can infer the model parameters as well as the latent states of the system accurately.

Algorithm 1 SAR Population Model Identification, Missing Value Imputation, and Outlier Detection

Input: $X_{\Omega_{x_i}}, U_{\Omega_{x_i}}, \eta_x, \eta_u \ \forall i \in \{1, \dots, N\}$

Output: $\boldsymbol{a}(s), \boldsymbol{b}(s), c(s), \hat{X}_i, \hat{U}_i,$
$\forall i \in \{1, \dots, N\}, \forall s \in \{1, \dots, S\}$

Randomly initialize $\boldsymbol{a}(s), \boldsymbol{b}(s), c(s), \sigma_i^2(\mathrm{s})$, and $p\left(s_t^i | s_{t-1}^i\right) \ \forall i \in \{1, \dots, N\}$

$k \leftarrow 0$

While $\|L_{k+1}(\theta) - L_k(\theta)\| > \varepsilon$

E-step: Estimate $\left(s_t^i\right) \forall i \in \{1, \dots, N\}, \forall t \in \{1, \dots, T\}$ by (19), and $p\left(s_t^i | s_{t-1}^i\right)$ by (20).

M-step: Optimize $\boldsymbol{a}(s), \boldsymbol{b}(s), c(s)$ by (23), and $\sigma_i^2(\mathrm{s})$ by (24)

For $i \in \{1, \dots, N\}$

Optimize $\hat{X}_i$: Select top η_x elements in
$\left(\hat{X}_i - X_i - \Delta g_{\hat{X}_i}\right)_{\Omega_{x_i}}$ forming the index set Z_{X_i}.

$\left(\hat{X}_i\right)_{\overline{\Omega}_{x_i} \cup Z_{X_i}} \leftarrow \left(\hat{X}_i - \Delta g_{\hat{X}_i}\right)_{\overline{\Omega}_{x_i} \cup Z_{X_i}}$

Optimize $\hat{U}_i$: Select top η_u elements in
$\left(\hat{U}_i - U_i - \Delta g_{\hat{U}_i}\right)_{\Omega_{u_i}}$ forming the index set Z_{U_i}.

$\left(\hat{U}_i\right)_{\overline{\Omega}_{u_i} \cup Z_{U_i}} \leftarrow \left(\hat{U}_i - \Delta g_{\hat{U}_i}\right)_{\overline{\Omega}_{u_i} \cup Z_{U_i}}$

End

$k \leftarrow k + 1$

End

Return $\boldsymbol{a}(s), \boldsymbol{b}(s), c(s), \hat{X}_i, \hat{U}_i,$
$\forall i \in \{1, \dots, N\}, \forall s \in \{1, \dots, S\}$

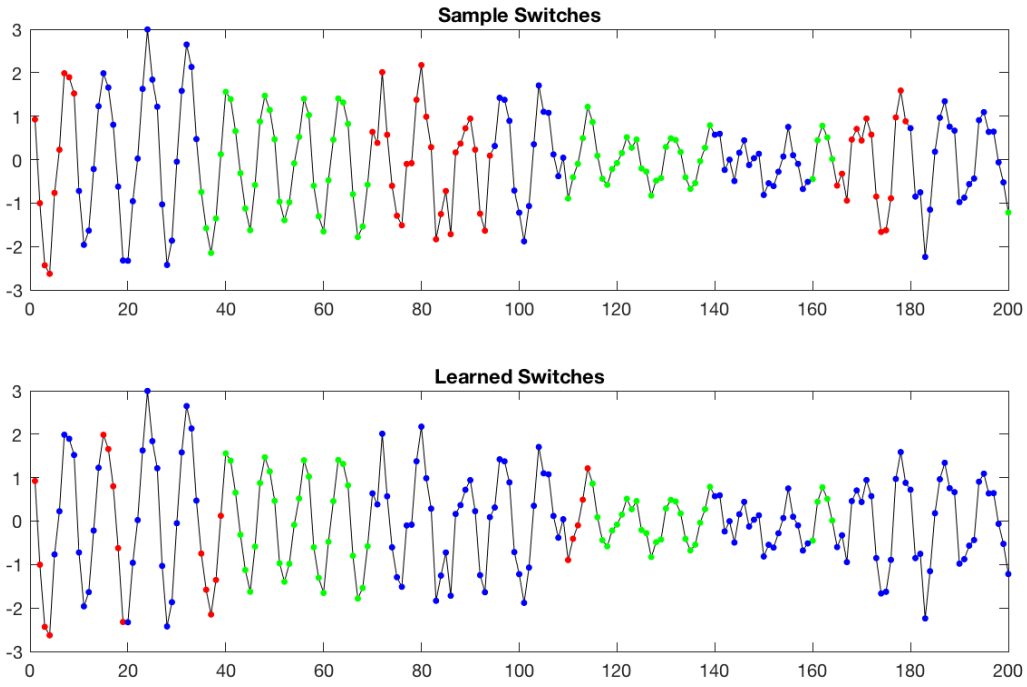

Figure 8. Inference of SAR model with 3 possible switching states

CHAPTER V

SWITCHING-STATE AUTO-REGRESSIVE POPULATION MODEL EVALUATION

We have implemented the population SAR model with the SSMO solution strategy on a real-world daily behavior dataset. This dataset consists of daily fitness behaviors of 25 different users. The dataset include diet, sleep, exercise information, and BMI collected from various sensor devices. In this dataset, almost all users show significant missing values and outliers, with patterns similar to Figure 1.

In our evaluation experiments, we first illustrate that integrating missing value imputation and outlier detection with model identification outperforms the common two-step procedure of data preprocessing and model identification. We then evaluate the SAR models with different complexity levels and identify an appropriate model for the population dynamics in the given data set. We benchmark different models and methods by conducting one-step ahead prediction of future BMI trajectory.

Missing Value and Outlier Detection Evaluation

The simultaneous missing value and outlier detection of our method have been tested against several analytic and off-the-shelf imputation and outlier detection methods. The methods we have compared include the mean value imputation, last value carried forward imputation, Principal Component Analysis (PCA) with B-spline bases [12], and PACE, a nonparametric Functional Principal Component Analysis (FPCA) method for sparse data [17]. The mean and last value carried forward imputation method is augmented with a median filter for outlier removal.

In our tests, the SAR population model with simultaneous imputation and outlier detection performs better than all the other methods we have benchmarked, giving the best prediction accuracy overall, as shown in Table 2. The analytic methods PACE and PCA with B-spline bases perform better than naive off-the-shelf methods, but our unified simultaneous imputation and outlier detection method clearly outperforms them. A comparison of our method and the analytic methods benchmarked for imputation and outlier detection is shown in Figure 9.

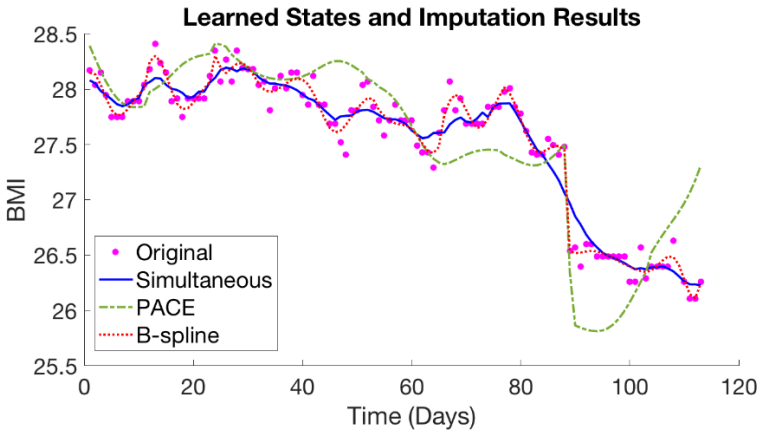

Figure 9. Missing value and outlier detection method comparison

Table 2: Evaluation result for different missing value estimation and outlier detection method

	Mean + Med	Last + Med	B-spline	PACE	**Simultaneous**
RMSE	0.72463 ± 0.53953	0.50286 ± 0.48841	0.46668 ± 0.48512	0.42348 ± 0.48489	**0.032114 ± 0.016565**
ABS	0.29995 ± 0.17872	0.17697 ± 0.12145	0.15886 ± 0.12179	0.11965 ± 0.10518	**0.024125 ± 0.011585**

Model Selection

We evaluate several different model parameters on the order of time lags of the state observations, L_x, the order on the input variables, L_u, as well as the number of states on the SAR model S. We find that the parsimonious setup that gives the best accuracy is where $L_x = L_u = 1$, while $S = 3$. The ABS prediction accuracy of different testing setups is shown in Table 3. In this

table, S1 denotes the one state model, reducing to the traditional AR model, S2 denotes the model with two latent states, and S3 denotes the model with three latent states. Increasing L_x, L_u, or S further did not yield any improvements in prediction accuracy.

Table 3: Absolute one-step-ahead prediction error of the SAR population model under different model parameters

		L_X = 1	L_X = 2	L_X = 3
L_U	1	S1: 0.045±0.030 S2: 0.029±0.013 **S3: 0.024±0.012**	S1: 0.072±0.027 S2: 0.037±0.016 S3: 0.059±0.056	S1: 0.084±0.030 S2: 0.052±0.024 S3: 0.074±0.072
	2	S1: 0.049±0.024 S2: 0.029±0.012 S3: 0.031±0.013	S1: 0.059±0.034 S2: 0.040±0.019 S3: 0.041±0.021	S1: 0.084±0.032 S2: 0.064±0.042 S3: 0.051±0.033
	3	S1: 0.056±0.023 S2: 0.041±0.015 S3: 0.037±0.026	S1: 0.068±0.026 S2: 0.040±0.017 S3: 0.074±0.072	S1: 0.096±0.060 S2: 0.064±0.044 S3: 0.045±0.030

The corresponding system coefficients obtained for the parsimonious model with the best prediction accuracy are shown in Table 4. For all three states, BMI would carry over to the next time point with very small changes, as the coefficients for BMI is close to one for all the states. On the other hand, the input variables that capture daily behavior influence have less significant contribution to current BMI when compared to the effects of previous BMI. This makes intuitive sense: The inherent BMI change dynamics should be relatively stable, while the input variables should only produce incremental changes to the previous BMI.

We conjecture that State 2 represents the most active state; State 1 represents the least active state, while State 3 is an intermediary state in between these two. We speculate this due to the following observations: First, note that the coefficient for BMI for State 2, denoted by $a(2)$, is the smallest followed by $a(3)$ and $a(1)$. Furthermore, $a(2) < 1$ and $a(1) > 1$. This means that without any external intervention as observable input variables, subjects in State 2 inherently lose weight the fastest while subjects in State 1 inherently gain weight. Second, we observe that with

increasing workout time, subjects in State 2 may have increasing BMI, but subjects in State 1 have decreasing BMI. We speculate that subjects in State 2 are gaining muscle mass while subjects in State 1 can better control their weight with more workout time.

The remaining coefficients also make sense intuitively. For example, for all the states, consuming food increases BMI while exercise helps control BMI.

Table 4: Normalized SAR coefficients for different variables under different states

Variable	State 1	State 2	State 3
BMI	1.0003	0.9824	0.9950
Exercise Calories	-0.0032	-0.0047	-0.0043
Food Calories	0.0007	0.0187	0.0104
Workout Calories	0.0031	-0.0080	0.0017
Workout Time	-0.0251	0.0261	0.0072

Prediction Accuracy Evaluation

We compare our model with the linear dynamic system model without switching states, denoted as SSMO [18]. Unlike our model, this model does not consider the potential heterogeneous dynamic changes in daily behavior data, and models each individual's dynamics with a different model instead of adopting a population model.

We benchmark the two models using both the L-1 norm absolute difference error (ABS) and the Residual Mean Squared Error (RMSE) in conducting one-step ahead prediction of future BMI trajectory. Our tests show that the SAR population model performs significantly better than SSMO as shown in Figure 10 and Table 5.

Table 5: Prediction accuracy comparison

	SSMO	SAR
ABS	0.22353 ± 0.28732	**0.024125 ± 0.011585**
RMSE	0.40324 ± 0.61404	**0.032114 ± 0.016565**

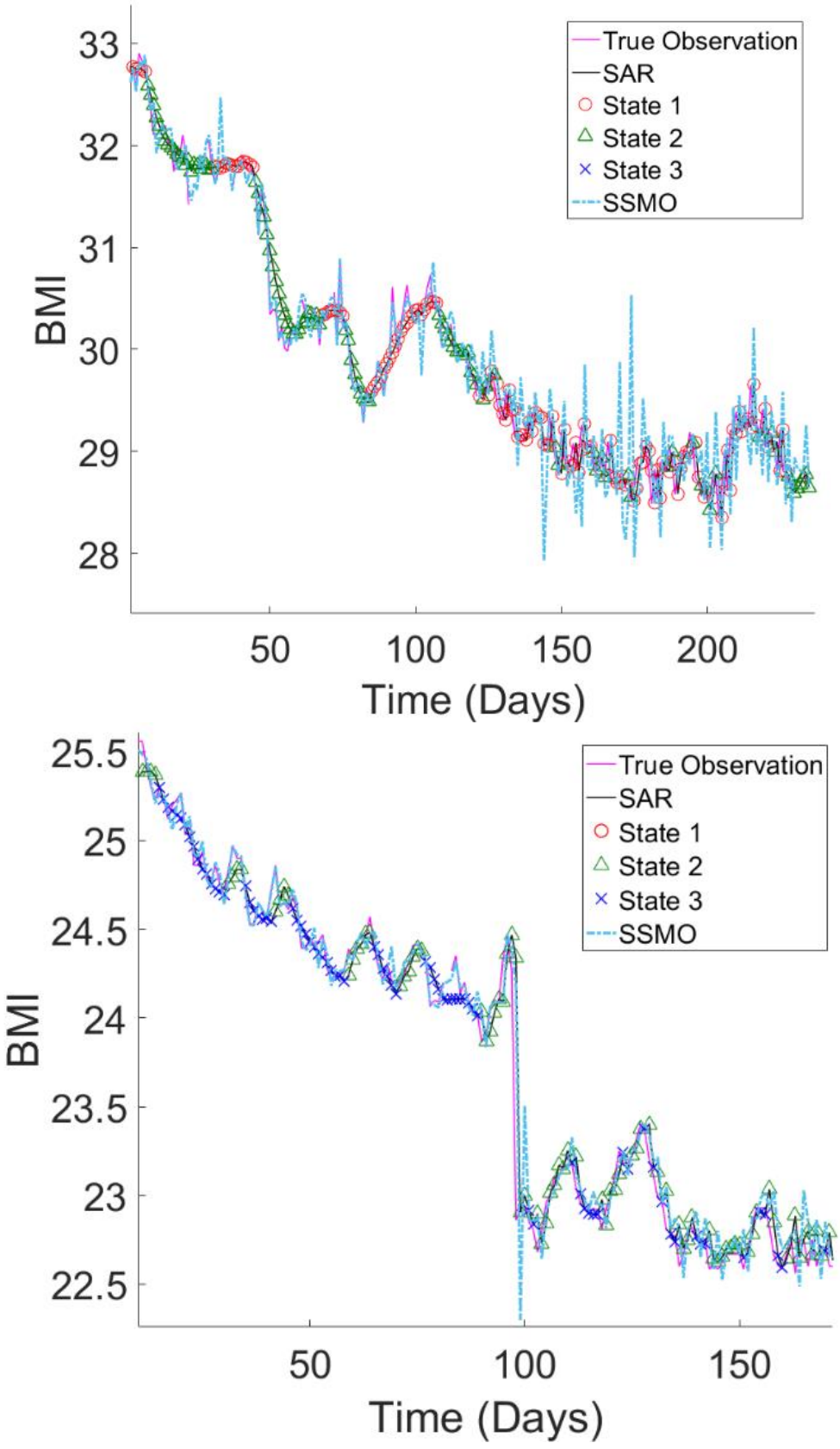

Figure 10. Prediction trajectory comparison

CHAPTER VI

INTERVENTION POLICY GENERATION USING GAUSSIAN PROCESS REINFORCEMENT LEARNING

Introduction

Using the learned model discussed in previous chapters, we propose an intervention framework that gives daily activity suggestions to control and specify user BMI at a desired level. To formulate this, a Reinforcement Learning (RL) method was adopted using Gaussian Processes (GP) to generalize the RL framework for continuous observation states and action variables. An advantage of Reinforcement Learning is that it does not require a detailed description of the underlying health dynamics [19]. Because of this, the method can be adopted to any model formulation such as the SAR population model described in previous chapters. On the other hand, non-parametric models such as Gaussian Processes eliminates the problem of model bias, making them a powerful tool for adaptive control [20].

Reinforcement Learning (RL)

Solving a RL problem consists of iteratively learning a task from interactions [19]. During learning, an agent interacts with the target system by taking an action $\mathbf{u}_t$, a combination of inputs that include variables such as calories to burn and calories to consume. The system then evolves from the state x_t to x_{t+1}, representing change in BMI. Assuming the SAR model formulation, the latent health state s_t also has a transition probability according to the underlying health dynamics. The agent receives a numerical signal r_t called the reward which provides a measure of how good the action taken at x_t was. This reward function can be defined as a Gaussian curve centered at the desired BMI level.

The objective of this method is to learn the optimal policy, $\boldsymbol{\pi}^*$, corresponding to the optimal intervention plan to set the user's BMI at the desired level. With this, the value function $V^{\boldsymbol{\pi}}(x)$ can be defined as the expected cumulative reward. As BMI regulation is a continuous task without a terminating state, a discounted sum of future rewards is used to define the expected state-value function as follows:

$$V^{\boldsymbol{\pi}}(x) = \mathrm{E}_{\boldsymbol{\pi}}[R_t|x_t = x] = \mathrm{E}_{\boldsymbol{\pi}}\left[\sum_{k}^{N} \gamma^k r_{t+k+1}\,|x_t = x\right] \quad (27)$$

Here, $\gamma \in (0,1]$ represents the discount factor while N is the number of simulated transitions of the system. Thus, the optimal state-value function is defined as follows:

$$V^*(x_t) = \max_{\mathbf{u}}\{r_t + \gamma \mathrm{E}_{x_{t+1}}[V^*(x_{t+1})|x_t, \mathbf{u}_t] \quad (28)$$

The state-action value function is defined by:

$$Q^*(x_t, \mathbf{u}_t) = r_t + \gamma \mathrm{E}_{x_{t+1}}[V^*(x_{t+1})|x_t, \mathbf{u}_t] \quad (29)$$

With the Q^* obtained, the optimal policy can be obtained directly as $\boldsymbol{\pi}^*(x_t) = \arg\max_{\mathbf{u}} Q^*(x, \mathbf{u})$.

In our problem, the states and actions are both continuously valued quantities. Thus, a function approximation technique is required for value function approximation. Gaussian process models are a powerful nonparametric method for generalizing reinforcement learning algorithms to continuous spaces.

Gaussian Process (GP)

A Gaussian Process is a generalization of a Gaussian probability distribution where the distribution is over functions instead of assuming a model with a given structure. To introduce this model, let $\mathbf{X}$: $\{\mathbf{x}_i \in \mathbb{R}^a | i = 1,2,\dots,n\}$ be the supporting input points while $\mathbf{Y}$: $\{\mathbf{y}_i \in \mathbb{R}^b | i = 1,2,\dots,n\}$ be the vector of corresponding output observations, while n is the number of observations. In this model, we assume that there is a functional relationship between inputs X and

outputs $\mathbf{Y}$ such that $\mathbf{y}_i = h(\mathbf{x}_i) + \varepsilon$, $\varepsilon \sim N(0, \sigma_\varepsilon^2)$. We can describe the inference of the function h by the posterior probability:

$$p(h|\mathbf{X},\mathbf{Y}) = \frac{p(\mathbf{Y}|h,\mathbf{X})p(h)}{p(\mathbf{Y}|\mathbf{X})} \quad (30)$$

Similar to a Gaussian distribution which can be represented by a mean vector and a covariance matrix, a GP can be modeled by a mean function and a covariance function as follows:

$$\boldsymbol{m}_h = \mathrm{E}[h(\mathbf{x}_t)] = Cov(\mathbf{x}_t,\mathbf{X}) + (\mathbf{K} + \sigma_\varepsilon^2\mathbf{I})^{-1}\mathbf{Y} \quad (31a)$$

$$Cov_h = \mathrm{Var}[h(\mathbf{x}_t)] = Cov(\mathbf{x}_t,\mathbf{x}_t) + Cov(\mathbf{x}_t,\mathbf{X})(\mathbf{K} + \sigma_\varepsilon^2\mathbf{I})^{-1}Cov(\mathbf{X},\mathbf{x}_t) \quad (31b)$$

Here, $\mathbf{K}$ is the kernel matrix with $\mathbf{K}_{ij} = Cov\left(\mathbf{x}_t^i,\mathbf{x}_t^j\right)\ \forall\, \mathbf{x}_t \in \mathbf{X}$. A common covariance function that we have adopted in our method is the squared exponential, denoted as follows:

$$Cov_{SE}\left(\mathbf{x}_t^i,\mathbf{x}_t^j\right) = \xi^2 \exp\left[-\frac{1}{2}\left(\mathbf{x}_t^i - \mathbf{x}_t^j\right)^{\mathrm{T}}\boldsymbol{\Lambda}\left(\mathbf{x}_t^i - \mathbf{x}_t^j\right)\right] \quad (32)$$

The parameters ξ and $\boldsymbol{\Lambda}$ are collected in a *hyperparameter* vector denoted by $\boldsymbol{\psi}$. The log-evidence is given as follows:

$$L = \log p(\mathbf{Y}|\mathbf{X},\boldsymbol{\psi}) = \int p(\mathbf{Y}, h(\mathbf{X}), \mathbf{X}, \boldsymbol{\psi})p(h(\mathbf{X})|\mathbf{X},\boldsymbol{\psi})dh$$

$$= -\frac{1}{2}\mathbf{Y}^{\mathrm{T}}(\mathbf{K} + \sigma_\varepsilon^2\mathbf{I})^{-1}\mathbf{Y} - \frac{1}{2}\log|(\mathbf{K} + \sigma_\varepsilon^2\mathbf{I})| - \frac{a}{2}\log 2\pi \quad (33)$$

Maximizing this quantity yields a functional model h that is nonparametric, rewards data and simplicity of the fitted model.

GP Modeling of the Value Function

To model the value function using a Gaussian process, the training targets can be generated by computing a discrete set of points $V(x_t)\ \forall t \in \{1, \dots, \tau\}$. On the other hand, the training inputs are $x_t\ \forall t \in \{1, \dots, \tau\}$. Similarly, the state-action value function $Q(x_t, \mathbf{u}_t)$ can be modeled by computing the points $Q(x_t, \mathbf{u}_t)\ \forall t \in \{1, \dots, \tau\}$ with the training inputs $x_t, \mathbf{u}_t\ \forall t \in \{1, \dots, \tau\}$. These

steps produce a GP approximation of the value function and the state-action value function, denoted by $V(\cdot)\sim GP_v(\boldsymbol{m}_v, Cov_v)$ and $Q(\cdot,\cdot)\sim GP_q(\boldsymbol{m}_q, Cov_q)$ respectively.

Using these values, the optimal action policy is given by the maximum of the mean function of GP_q. This is obtained by solving the following optimization problem:

$$\boldsymbol{\pi}^*(x_t) = \underset{\mathbf{u}}{\operatorname{argmax}}\, Q^*(x_t, \mathbf{u}) = \underset{\mathbf{u}}{\operatorname{argmax}}\, m_q(\mathbf{u}) \quad (34)$$

Noting the potential non-convexity of this optimization problem, we utilize a simulated annealing approach in obtaining a global maximum [21]. The entire Gaussian Process Reinforcement Learning (RLGP) procedure is described in Algorithm 3.

Algorithm 3 Reinforcement Learning Gaussian Process

Inputs:
Model Parameters: x_0, θ
RL Parameters: $r(\cdot), \tau, \gamma, \varepsilon, N$
$k \leftarrow 0$
Randomly initialize $\boldsymbol{\pi}_0$
While $\|L_{k+1} - L_k\| > \varepsilon$
$k \leftarrow k + 1$
Simulate τ transitions using the model θ, applying $\mathbf{u}_t \ \forall t \in \{1, \dots, \tau\}$ from $\boldsymbol{\pi}_{k-1}$
$\{r_t\}_{t=1}^{t=\tau} \leftarrow \{r(x_t)\}_{t=1}^{t=\tau}$
Estimate $V(x_t) \ \forall t \in \{1, \dots, \tau\}$ by (27)
Approximate $V(\cdot)\sim GP_v$ with $V(x_t)$ and $x_t \ \forall t \in \{1, \dots, \tau\}$
For $\forall i \in \{1, \dots, \tau\}$
For $\forall n \in \{1, \dots, N\}$
For each $j \in \{1, \dots, U\}$, randomly sample u_t^j from $t \in \{1, \dots, \tau\}$ forming $\mathbf{u}_n$
$Q(x_i, \mathbf{u}_n) = r(x_i, \mathbf{u}_n) + \gamma E[V(x_i')|x_i, \mathbf{u}_n, \theta, GP_v]$
End
$Q(x_i,\cdot)\sim GP_q$ with $Q(x_i, \mathbf{u}_n)$ and $\mathbf{u}_n \ \forall n \in \{1, \dots, N\}$
$\boldsymbol{\pi}^*(x_i) = \underset{\mathbf{u}}{\operatorname{argmax}}\, Q^*(x_i, \mathbf{u}) = \underset{\mathbf{u}}{\operatorname{argmax}}\, m_q(\mathbf{u})$
End
$\boldsymbol{\pi}^*(\mathrm{X}) = \{\boldsymbol{\pi}^*(x_i)\} \ \forall i \in \{1, \dots, \tau\}$
Approximate $\boldsymbol{\pi}_k(\cdot)\sim GP_{\boldsymbol{\pi}_k}$ with $\boldsymbol{\pi}^*(\mathrm{X})$ and $x_i \ \forall i \in \{1, \dots, \tau\}$
Calculate L_k by (33)
End
Return $\boldsymbol{\pi}^* = \boldsymbol{\pi}_k \sim GP_{\boldsymbol{\pi}_k}$

CHAPTER VII

CONCLUSION

We have implemented and carried out comprehensive evaluation of population Switching-state Auto-Regressive (SAR) models together with missing value imputation and outlier detection on real-world daily behavioral data. Different from the existing common procedure of imputation and outlier detection as separated data preprocessing step when analyzing behavioral sensor data, we handle missing data and outliers by simultaneously considering them while conducting model identification. We have conducted model selection to obtain the most accurate and parsimonious representation of the given data set and have shown that the identified model makes intuitive sense.

From our evaluation experiments, conducting missing value imputation and outlier detection while simultaneously identifying the model significantly improves model accuracy when compared with methods that firstly preprocess the data. In addition, we show that considering population-wide effects and dynamic heterogeneity significantly improves prediction performance on our data set.

As the dynamics of human behavior data has been largely an uncharted research territory, characterizing the science of these unknown dynamics demands more in-depth study of the principles and complex relationships among the health outcomes and their control variables. By understanding these relationships, we plan to derive an automatic health intervention framework using the learned daily behavioral health model. Ultimately, integration of these highly analytic models in real-world clinical implementation demands collaboration with systems engineering and health implementation science to ensure optimal patient treatment.

REFERENCES

[1] D. Barber, *Bayesian reasoning and machine learning*: Cambridge University Press, 2012.

[2] J. Bibby, J. Kent, and K. Mardia, "Multivariate analysis," ed: Academic Press, London, 1979.

[3] G. E. Box, G. M. Jenkins, G. C. Reinsel, and G. M. Ljung, *Time series analysis: forecasting and control*: John Wiley & Sons, 2015.

[4] S. Boyd and L. Vandenberghe, *Convex optimization*: Cambridge university press, 2004.

[5] S. Consolvo, D. W. McDonald, T. Toscos, M. Y. Chen, J. Froehlich, B. Harrison, et al., "Activity sensing in the wild: a field trial of ubifit garden," in *Proceedings of the SIGCHI Conference on Human Factors in Computing Systems*, 2008, pp. 1797-1806.

[6] L. Debnath and F. A. Shah, *Wavelet transforms and their applications*: Springer, 2002.

[7] J. Durbin and S. J. Koopman, *Time series analysis by state space methods* vol. 38: OUP Oxford, 2012.

[8] A. Gelman and J. Hill, *Data analysis using regression and multilevel/hierarchical models*: Cambridge university press, 2006.

[9] C. L. Ogden, M. D. Carroll, B. K. Kit, and K. M. Flegal, "Prevalence of childhood and adult obesity in the United States, 2011-2012," Jama, vol. 311, pp. 806-814, 2014.

[10] M. B. Priestley, "Spectral analysis and time series," 1981.

[11] L. R. Rabiner, "A tutorial on hidden Markov models and selected applications in speech recognition," *Proceedings of the IEEE*, vol. 77, pp. 257-286, 1989.

[12] J. O. Ramsay, *Functional data analysis*: Wiley Online Library, 2006.

[13] G. P. Rodgers and F. S. Collins, "The next generation of obesity research: no time to waste," *Jama*, vol. 308, pp. 1095-1096, 2012.

[14] R. Somasundaram and R. Nedunchezhian, "Evaluation of three simple imputation methods for enhancing preprocessing of data with missing values," *International Journal of Computer Applications*, Vol21, vol. 10, 2011.

[15] P. Tseng, "Convergence of a block coordinate descent method for nondifferentiable minimization," *Journal of optimization theory and applications*, vol. 109, pp. 475-494, 2001.

[16] W. A. Woodward, H. L. Gray, and A. C. Elliott, *Applied time series analysis*: CRC press, 2011.

[17] F. Yao, H.-G. Müller, and J.-L. Wang, "Functional data analysis for sparse longitudinal data," *Journal of the American Statistical Association*, vol. 100, pp. 577-590, 2005.

[18] C. Xiao, S. Gui, Y. Cheng, X. Qian, J. Liu, and S. Huang, "Learning Longitudinal Planning for Personalized Health Management from Daily Behavioral Data", in submission, 2016.

[19] M. E. Harmon and S. S. Harmon, "Reinforcement learning: A tutorial," *WL/AAFC, WPAFB Ohio*, vol. 45433, 1996.

[20] C. E. Rasmussen, "Gaussian processes for machine learning," 2006.

[21] S. Kirkpatrick, C. D. Gelatt, and M. P. Vecchi, "Optimization by simulated annealing," *science*, vol. 220, pp. 671-680, 1983.